Automatic segmentation and parameter estimation of the lower tear meniscus

Hannes Stegmann[1,2], Valentin Aranha dos Santos[1,2], Martin Pfister[1,2], Alina Messner[1], Angelika Unterhuber[1], Gerhard Garhöfer[3], Leopold Schmetterer[1-6] and René M. Werkmeister[1,2]

[1] Center for Medical Physics and Biomedical Engineering, Medical University of Vienna, Austria
[2] Christian Doppler Laboratory for Ocular and Dermal Effects of Thiomers, Medical University of Vienna, Austria
[3] Department of Clinical Pharmacology, Medical University of Vienna, Austria
[4] Singapore Eye Research Institute, Singapore National Eye Centre, Singapore
[5] Lee Kong Chian School of Medicine, Nanyang Technological University, Singapore
[6] Ophthalmology and Visual Sciences Academic Clinical Program, Duke-NUS Medical School, Singapore

Objective

To automatically estimate potential biomarkers of the lower tear meniscus from acquired UHR-OCT images. These parameters could be used in the future to help with the diagnosis and treatment of tear film related diseases like dry eye disease (DED).

Subjects and image acquisition

The tear meniscus measurements were obtained from ten healthy subjects (five female, five male, age 31 ± 10 years, mean ± SD). The images are taken from a volume centered on the lower eyelid margin that covers 2.9 x 4 x 2 mm^3 (height x width x depth, in air). The measurements were acquired with a custom-built ultrahigh-resolution (UHR-)OCT system with a lateral resolution of 21 µm and an axial resolution of 1.2 µm in tissue.

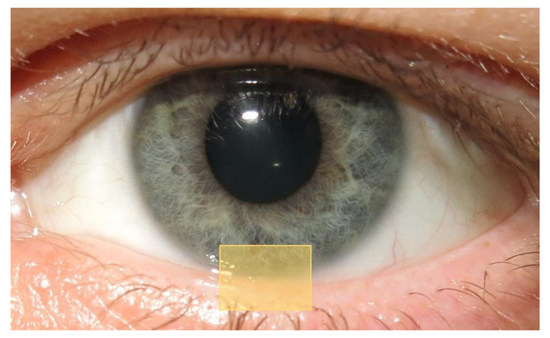

Fig 1. Measurement region of the lower tear meniscus.

Threshold-based segmentation (TBSA)

The first segmentation algorithm is based on thresholding and the detection of the tear meniscus contour (not shown). Based on the segmentation, the algorithm extracts four tear meniscus parameters: tear meniscus area (TMA), tear meniscus height (TMH), tear meniscus depth (TMD) and radius of curvature (TMR).

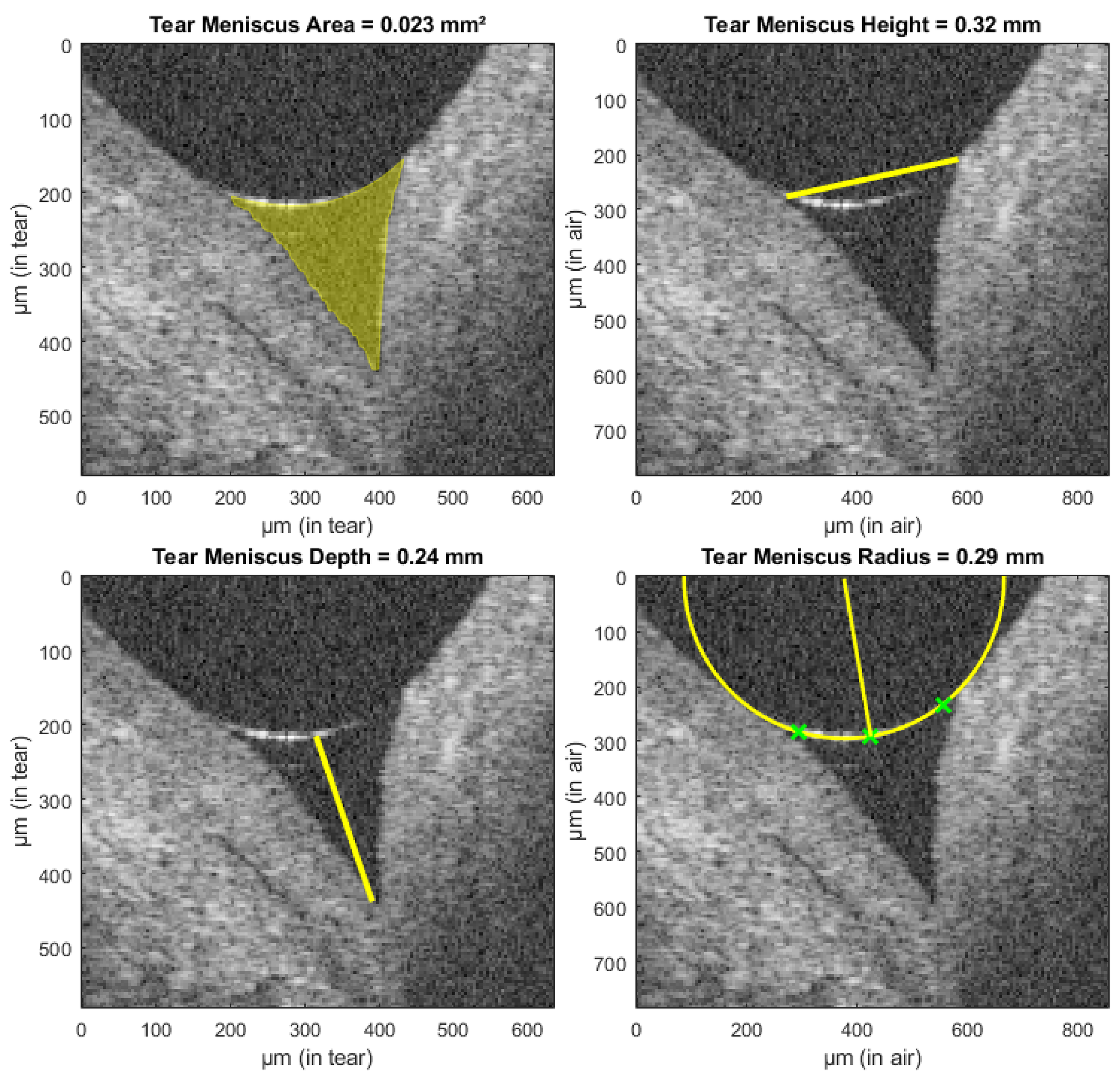

Fig. 2 - Automatic segmentation of the lower tear meniscus in a healthy subject. Estimated parameters are TMA, TMH, TMD and TMR [1].

Neural network segmentation (DSA & LSA)

We created a dataset consisting of 6658 images, where the correct segmentation of the TMA was visually confirmed by an experienced operator and subsequently used as a ground-truth mask. We also used an intermediate result of the TBSA, which provides the bounding box coordinates of the tear meniscus.

This dataset was used to train two different neural network approaches: the **direct segmentation approach (DSA)**, where the image is directly used as input after rescaling, and the **localized segmentation approach (LSA)**, where two neural networks work in cascade and only a detected region of interest is segmented. The latter is of interest because the dataset has a low tear meniscus support of only 0.71%, which can make the training difficult. In both cases the segmentation is done with highly similar networks, which only differ in their input dimensions. The network of the localization is very simple and has only a single convolution layer (not shown), but manages to generate a bounding box that contains on average 99.99 % of all tear meniscus pixels.

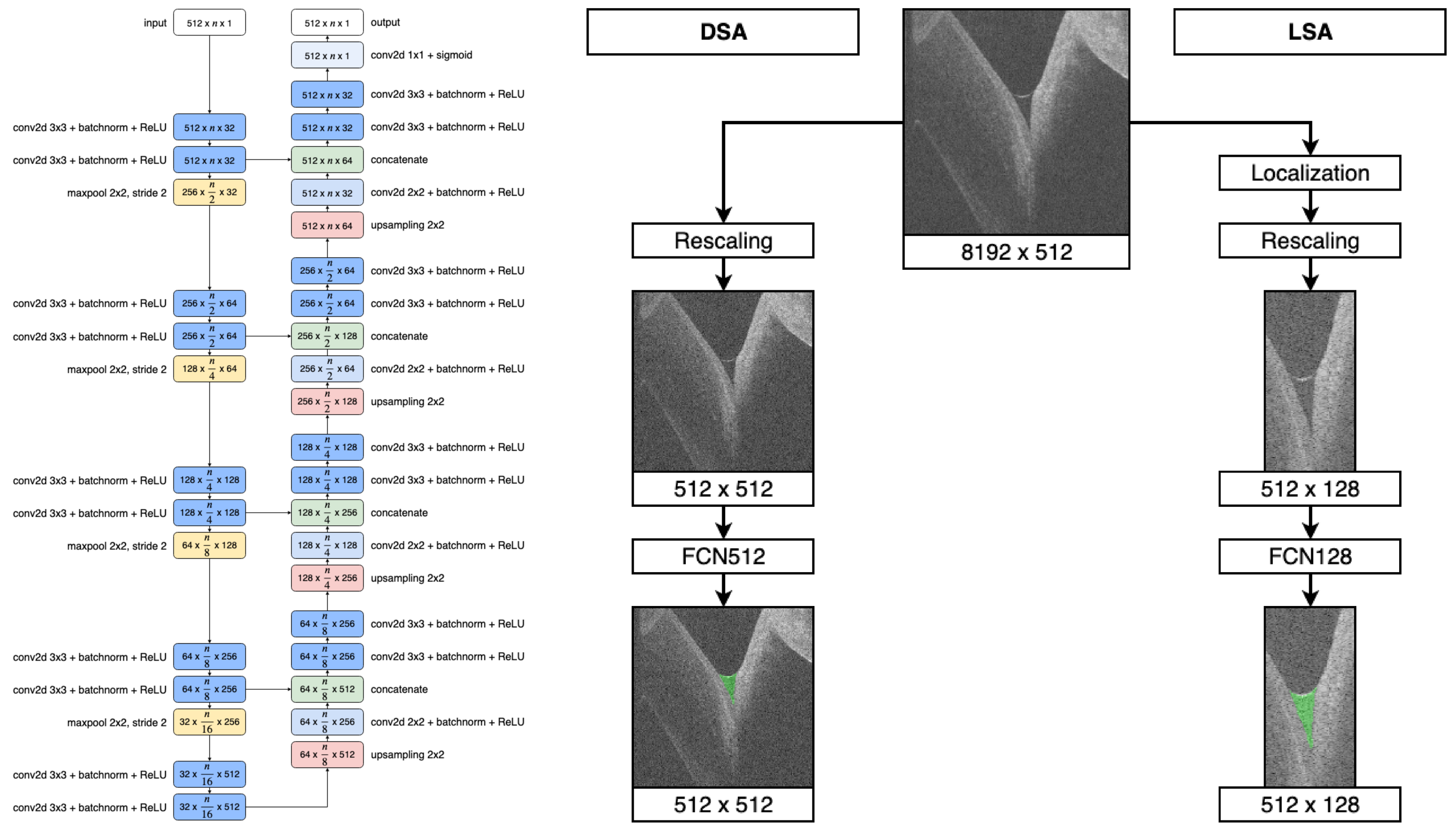

Fig. 3 – Left: U-Net-like architectures of the segmentation networks, which only differ in their input dimension *n*. Right: Segmentation workflow of the two compared approaches. For FCN512, *n*=512 and for FCN 128, *n*=128. [2]

Table 1 – Comparison of the five-fold cross-validated performance metrics of both approaches. The values are averaged over all folds and weighted by the number of images in the fold.

Approach		Support	Jaccard	Dice	Accuracy	Sensitivity	Specificity
DSA	mean	0.0071	0.9324	0.9644	0.9995	0.9636	0.9998
	± std	± 0.0021	± 0.0432	± 0.0261	± 0.0003	± 0.0361	± 0.0001
LSA	mean	0.0418	0.9316	0.9638	0.9972	0.9643	0.9986
	± std	± 0.0136	± 0.0474	± 0.0318	± 0.0027	± 0.0262	± 0.0024

Comparison in challenging cases

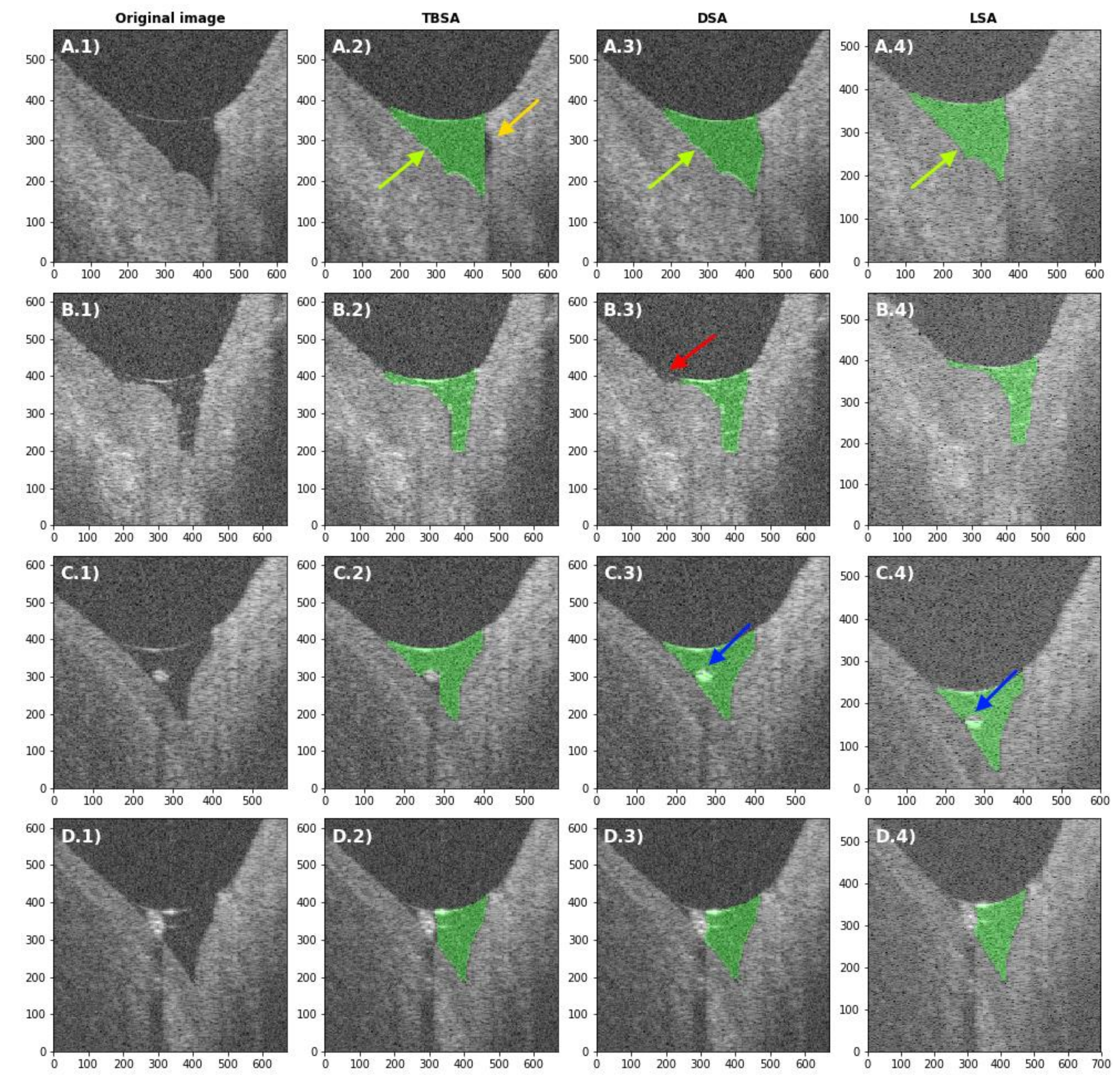

Fig. 4 Rare and challenging segmentation tasks (1). None of the images were part of the training dataset. (A) Not segmented lateral cavity (orange arrow), (B) irregular meniscus shape, (C) small debris and (D) larger debris cutting the tear meniscus area in two parts. Green arrow: example areas where the bordering pixels are included in or excluded from the tear meniscus area. Red arrow: non-segmented region of the tear meniscus area. Blue arrow: holes in the segmented area, where debris is present. The axes represent µm in tear fluid. [2]

Conclusion

UHR-OCT cross-sectional images of the lower eyelid margin can be used to extract a wide variety of tear meniscus parameters, which can help with the investigation of tear film related diseases in a clinical setting. Deep learning segmentation can be used to further improve the segmentation, not only in regards to processing speed. Both DSA and LSA perform very well, with the LSA showing more potential for the segmentation of challenging cases, where it outperforms TBSA and DSA. Yet, large debris still poses a challenge. In the future, the dataset could be improved by including data from non-healthy cases and measurements acquired with different OCT systems.

References

[1] Stegmann et al., *Automatic assessment of tear film and tear meniscus parameters in healthy subjects using ultrahigh-resolution optical coherence tomography,* Biomed. Opt. Express 10(6), p. 2744–2756 (2019).
[2] Stegmann et al., *Deep learning segmentation for optical coherence tomography measurements of the lower tear meniscus,* Biomed. Opt. Express 11, p. 1539-1554 (2020)

contact: hannes.stegmann@meduniwien.ac.at